

MOLECULAR DYNAMICS SIMULATIONS ON THE INTERLEUKIN-1 $\beta$ :INTERLEUKIN  
RECEPTOR I:INTERLEUKIN-1 RECEPTOR ACCESSORY PROTEIN TERNARY  
COMPLEX

by

Reva Joshi  
A Thesis  
Submitted to the  
Graduate Faculty  
of  
George Mason University  
in Partial Fulfillment of  
The Requirements for the Degree  
of  
Master of Science  
Biochemistry

Committee:

\_\_\_\_\_

Dr. Mikell Paige, Thesis Director and  
Committee Member

\_\_\_\_\_

Dr. Barney Bishop, Committee Member

\_\_\_\_\_

Dr. Young-Ok You, Committee Member

\_\_\_\_\_

Dr. Gerald Weatherspoon, Department  
Chairperson

\_\_\_\_\_

Dr. Donna M. Fox, Associate Dean, Office  
of Student Affairs & Special Programs,  
College of Science

\_\_\_\_\_

Dr. Peggy Agouris, Dean, College of  
Science

Date: \_\_\_\_\_

Summer Semester 2018  
George Mason University  
Fairfax, VA

Molecular Dynamics Simulations on the Interleukin-1 $\beta$ :Interleukin Receptor  
I:Interleukin-1 Receptor Accessory Protein Ternary Complex

A Thesis submitted in partial fulfillment of the requirements for the degree of  
Master of Science at George Mason University

by

Reva Joshi  
Bachelor of Science  
Virginia Commonwealth University, 2016

Director: Mikell Paige, PhD.  
Associate Professor  
George Mason University

Summer Semester 2018  
George Mason University  
Fairfax, VA

## *Acknowledgements*

I would like to thank Dr. Paige all his support and advice over the past year and a half. I would also like to thank my friends here at GMU who kept me sane during the stressful periods. And lastly, thank you to my family for everything in my entire life.

## *Table of Contents*

List of Tables.....	iv
List of Figures.....	vi
List of Equations.....	vii
Abstract .....	vii
Interleukin-1 $\beta$ .....	1
Molecular Dynamics .....	4
Time Dependence.....	5
Statistical Ensemble .....	5
Potential Energy Function .....	6
Amber MD .....	7
Molecular Mechanics – Poisson-Boltzmann and Generalized Born Surface Area.....	7
Fragment Molecular Orbital Theory.....	9
Pair Interaction Energy Decomposition Analysis.....	10
QM Calculations .....	11
Facio FMO and GAMESS.....	12
Results.....	13
MD Simulation Stability .....	13
MM-PBSA/GBSA Results.....	17
FMO Results.....	20
Hydrogen Bond Analysis .....	21
Conclusion .....	23
Methods.....	24
Hardware/Software .....	24
Initial Editing.....	25
MD and MM-PBSA/GBSA in Amber .....	25

FMO and GAMESS.....	26
Appendix.....	28
References.....	32

## *List of Tables*

1. Binding regions and specific residues belonging to each. .... 19
2. Residues belonging to pairs 1-5..... 21

## *List of Figures*

1. Interleukin-1 $\beta$ ternary complex; IL-1 $\beta$ in light grey, IL-1RI in medium grey, IL-1RAcP in dark grey.....	2
2. Visual representation of the manner in which the MM-PBSA/GBSA program calculates free energy of binding.....	8
3. Fragment used in FMO calculations, including Arg-286 and local residues within 0.5 nm.....	10
4. Root-mean-square deviation across total simulation time.....	14
5. Coefficient of variation in RMSD across total simulation time. ....	14
6. Radius of gyration across total simulation time.....	15
7. Coefficient of variation in radius of gyration across total simulation time.....	15
8. Average root-mean-square fluctuation for each residue throughout total simulation time.....	16
9. Potential energy across total simulation time.....	17
10. Coefficient of variation in potential energy across total simulation time. ....	17
11. Decomposed free energy of binding for region I-IV residues. ....	19
12. Total free energy of binding for region I-IV residues. ....	19
13. Decomposed pair interaction energy for pairs 1-5. ....	21
14. Total pair interaction energy for pairs 1-5.....	21
15. Hydrogen bond between Arg-286 (IL-1RAcP) and Asp-54 (IL-1 $\beta$ ) as identified in Chimera. ....	22

*List of Equations*

1. Lennard-Jones Potential Energy Function.....	6
2. Free Energy of Binding.....	7
3. Interaction Energy .....	11
4. Schrödinger Equation .....	11
5. Free Energy of Binding (Parts of Energy) .....	18



## *Abstract*

### MOLECULAR DYNAMICS SIMULATIONS ON THE INTERLEUKIN-1 $\beta$ :INTERLEUKIN RECEPTOR I:INTERLEUKIN-1 RECEPTOR ACCESSORY PROTEIN TERNARY COMPLEX

Reva Joshi, M.S.

George Mason University

Thesis Director: Dr. Mikell Paige

Osteoarthritis affects millions of people worldwide each year. The inflammatory signaling pathway associated with osteoarthritis contains a possible novel drug target, the IL-1 $\beta$  ternary complex. IL-1 $\beta$  interacts with two associated proteins, IL-1RI and IL-1RAcP, to exert downstream inflammatory effects. Experimental studies of this complex have identified residue Arg-286 of IL-1RAcP as a “hot spot” of interaction. This paper aimed to computationally study the IL-1 $\beta$  complex with molecular mechanical and quantum mechanical methods. The study found Arg-286 of IL-1RAcP to be the hot spot, participating in a hydrogen bond with Asp-54 of IL-

1 $\beta$ . In agreement with previous experimental studies, Arg-286 was identified as a possible target for drug discovery aimed at inhibiting IL-1 $\beta$  complex and its ultimate downstream inflammatory effects.

## ***Interleukin-1 $\beta$***

Osteoarthritis is a chronic degenerative disease that effects millions of people each year worldwide. Osteoarthritis, the most common type of arthritis, erodes the cartilage in joints, causing pain and immobility. Osteoarthritis commonly affects the hands, knees, hips, and spine, and is thought to be the result of mechanical stress and inflammation. There is currently no cure for osteoarthritis and the medications used to relieve the symptoms are associated with serious adverse side-effects. Designing a drug specific to the signaling cascade present in osteoarthritis could result in a more effective and targeted therapeutic strategy that can circumvent the negative side effects.

Interleukin-1 $\beta$  (IL-1 $\beta$ ) is an immune system signaling protein implicated in osteoarthritis inflammatory signaling cascade. IL-1 $\beta$  is a proinflammatory cytokine that functions through interactions with the interleukin-1 receptor I (IL-1RI) and interleukin-1 receptor-Accessory Protein (IL-1RAcP). IL-1 $\beta$  offers a novel target for osteoarthritic drug design, thus studying the IL-1 $\beta$  ternary complex interaction can lead to the rational design of a new drug to prevent and combat osteoarthritis.

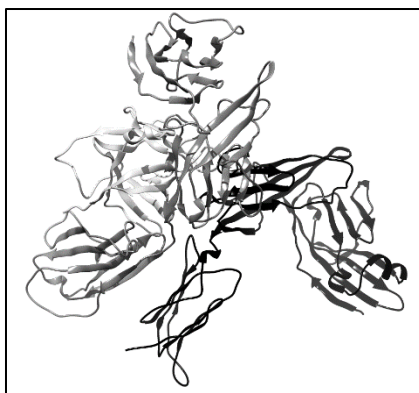


Figure 1. Interleukin-1 $\beta$  ternary complex; IL-1 $\beta$  in light grey, IL-1RI in medium grey, IL-1RAcP in dark grey.

The x-ray crystal structure for the IL-1 $\beta$  ternary complex was solved in 2014 at Stanford University by Christoph Thomas and co-workers, wherein the residues on the protein interfaces that may contribute to protein interaction were identified. More recently, a study done by Dr. Alessandra Luchini and Dr. Lance Liotta at the Center for Applied Proteomics and Molecular Medicine (CAPMM) at George Mason University identified a “hot spot” for the protein complex interaction. The Arg-286 residue of the IL-1RAcP protein was identified as a key hot spot residue. Site-directed mutagenesis of the Arg-286 residue validated the importance of this residue for the protein-protein interaction.

This study aims to computationally study the ternary complex interaction to identify hot spots via modelling and determine interactions critical to binding and

activity through classical and quantum mechanical calculations. The results garnered from this study will offer a deeper understanding of the protein-protein interactions and possibly provide an explanation for the experimental results.

## ***Molecular Dynamics***

Molecular dynamics (MD) is a widely used tool in the chemical and physical study of biomolecules. MD software generates simulations of proteins, allowing them to move and interact as if in their native environment. Simulations alone can provide detailed information on molecular motions that are inaccessible in any other way. In addition to simulations, molecular mechanics calculations can be performed to determine several important properties such as free energy of binding.

There are two approaches to studying proteins, outside of computational chemistry, that provide pieces to understanding protein structure and function. Experimental protein assays can be used to study protein function and X-ray crystallography can be used to solve the protein structure with atomistic resolution. MD can be useful in tying protein structure and function together by visually and quantitatively studying the dynamics of protein interaction based on X-ray crystal structures, and then comparing to experimental results.

Molecular mechanics (MM), the basis of MD, involves simplifying the model of the atom to fit classical mechanics. While this model is not perfect, it can be used to accurately estimate molecular motion. In molecular mechanics, each atom is treated

as a charged ball and each bond is treated as a spring. When the temperature of the system is slowly raised, the charged balls begin to move, and the motion is propagated across the entire protein via the springs. MD and MM are nearly synonymous, the only difference being time-dependence. MD shows molecular motion evolving over time, while MM refers to an instantaneous calculation.

Three key features of MD simulations are discussed below, including time-dependence, statistical ensembles, and the potential energy function.

### *Time Dependence*

Time-dependence is a critical component of MD simulations. At each set time step, force and energy are calculated for each atom and new coordinates are written. In the case of most simulations, this time step is 1-2 femtoseconds ( $10^{-15}$  seconds). Ultimately, when several thousand frames are calculated and drawn, they are put together to show molecular motion with respect to time on the scale of nanoseconds ( $10^{-9}$  seconds). The accumulation of 20 nanoseconds of data is a standard in the literature to assume equilibration of the system.

### *Statistical Ensemble*

There are several commonly used ensembles in MD that account for different simulation conditions. For example, the canonical, or NVT ensemble, is initially used to introduce temperature and minimize total energy of a protein system. The acronym NVT represent the values held constant in this ensemble – N (number of particles), V (volume), and T (temperature). The NVT ensemble is used to heat the

system to 300 K prior to pressure scaling because calculating and maintaining constant pressure at low temperatures can lead to inaccuracies and instability. Additionally, the isobaric-isothermal, or NPT ensemble, is used to equilibrate density in protein systems after NVT equilibration. The acronym NPT represents the values held constant in this type of ensemble – N (number of particles), P (pressure), and T (temperature). Langevin temperature and Berendsen pressure scaling methods are used to determine temperature and pressure, then make small-scale adjustments to the system to ensure constancy over time. The NPT ensemble allows the potential energy of the system to stabilize progressively, thus generating a set of structural configurations that represent the presumed native structure of the protein.

### *Potential Energy Function*

The potential energy (PE) of each atom is calculated by determining atom pair interaction energy via the Lennard-Jones potential energy function,

$$V_{LJ} = 4\varepsilon \left[ \left( \frac{\sigma}{r} \right)^{12} - \left( \frac{\sigma}{r} \right)^6 \right] = \varepsilon \left[ \left( \frac{r_m}{r} \right)^{12} - 2 \left( \frac{r_m}{r} \right)^6 \right] \quad (1)$$

where  $\varepsilon$  is the depth of the potential well,  $\sigma$  is the interatomic distance at which the PE is zero,  $r$  is actual interatomic distance, and  $r_m$  is the interatomic distance at PE minimum. Force, the spatial derivative of potential energy, is then calculated and Newton's laws of motion determine how the forces on each atom impact their position and velocity.



### *Amber MD*

There are many commercially available software packages that perform molecular dynamics simulations. Among the most popular and widely used is Amber MD. The most important piece of these software packages are the force fields they come equipped with. A force field is a set of equations and parameters that calculate force and energy and draw coordinates. Amber force fields have been developed over several generations from the first, Amber99 to the latest, Amber18. Force fields are tested against experimental data and are continuously refined and improved. Among Amber's capabilities are programs that prepare and solvate molecules, run simulations, and analyze simulations.

### *Molecular Mechanics – Poisson-Boltzmann and Generalized Born Surface Area*

One such analyzing tool, Molecular Mechanics – Poisson Boltzmann and Generalized Born Surface Area (MM-PBSA/GBSA), is used to determine free energy of binding between a protein and ligand. This method works by calculating electrostatic energy of the protein and ligand in bound and unbound states, then removing the solvation energy, to ultimately solve for free energy of binding. This calculation, in its simplified form,

$$\Delta G_{bind} = \Delta E_{MM} + (\Delta G_{solv}^{complex} - \Delta G_{solv}^{receptor} - \Delta G_{solv}^{ligand}) - T\Delta S_{config} \quad (2)$$

where  $\Delta G$  is free energy,  $\Delta E_{MM}$  is electrostatic energy,  $T$  is temperature, and  $\Delta S$  is change in entropy, coincides with figure 2. The free energy of binding can also be

decomposed into per-residue free energy of binding to determine which residues contribute most to binding.

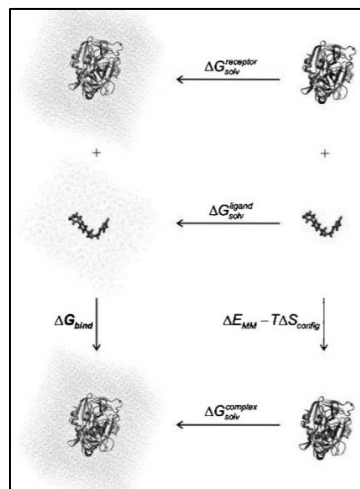


Figure 2. Visual representation of the manner in which the MM-PBSA/GBSA program calculates free energy of binding.

To apply this method to a ternary complex, two proteins, IL-1 $\beta$  and IL-1RI, were labeled the 'protein' and IL-1RAcP was labeled the ligand.

### ***Fragment Molecular Orbital Theory***

While MM and MD provide a good approximation using classical mechanics, the assumptions associated with such methods simplify the true intricacy of protein interactions. MM can resolve electrostatic interactions and hydrogen bonding but not dipole or dispersion forces, which contribute to binding. Instead, these van der Waals forces can be studied using quantum mechanical (QM) calculations. QM studies on large protein structures, however, would be too computationally intensive and therefore impractical. To make these calculations feasible, the Fragment Molecular Orbital method was used.

The Fragment Molecular Orbital (FMO) method applies QM calculations to a small subsection of a protein system. A portion of a larger protein system is isolated and broken down into fragments no larger than dimers. Then, QM calculations can be applied to the system of fragments to ultimately study protein interaction.

FMO method is predicated on the notion that all chemistry is local. Therefore, any significant interactions recognized by QM studies of the whole protein will also be present in calculations of a portion of that protein. By reducing the number of

atoms in the calculation, FMO provides a practical method of applying QM on proteins within reasonable computational and time restrictions.

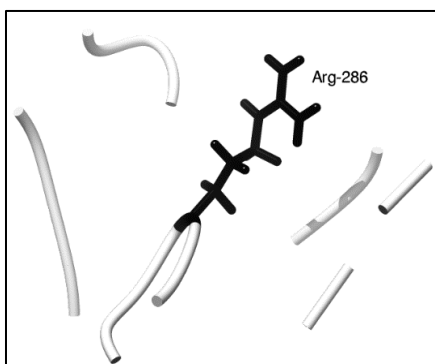


Figure 3. Fragment used in FMO calculations, including Arg-286 and local residues within 0.5 nm.

A specific tool in FMO, pair interaction energy decomposition analysis (PIEDA), is used to determine interaction energy between pairs of protein fragments.

#### *Pair Interaction Energy Decomposition Analysis*

PIEDA works by calculating interaction energy for all possible fragment pairs. Then, to study the critical interactions, total interaction energy is decomposed into its components. PIEDA is performed by solving for electrostatic (ES), exchange

repulsion (EX), and dispersion energy (DI) separately. Then, charge transfer energy (CT) and the mixed term contribution account for the remainder of total energy.

$$\Delta E^{int} = \Delta E^{es} + \Delta E^{di} + \Delta E^{ct} + \Delta E^{ex} \quad (3)$$

PIEDA is the FMO equivalent of energy decomposition analysis (EDA) used for non-covalently bound molecules. EDA was remodeled to solve for pair interaction energy for fragments in FMO with the same energy decomposition functionality.

#### *QM Calculations*

In general, QM calculations involve solving the Schrödinger equation,

$$\hat{H}\Psi = E\Psi \quad (4)$$

where  $\hat{H}$  is the Hamiltonian operator,  $\Psi$  is the wave function, and  $E$  is the energy. Specifically, our calculations were performed using the Restricted Hartree-Fock (RHF) method and the 6-31G basis set. The RHF method, also known as the self-consistent field (SCF) method, approximates the Hamiltonian then iteratively solves the Schrödinger equation to achieve a more accurate set of orbitals until the results converge. The approximation involves simplifying the system in mathematical terms such that the Schrödinger equation may be solved for a multi-electron system, which otherwise has no known solutions. Basis sets contain initial atomic orbitals upon which approximation via the RHF method can occur. The 6-31G basis set is a moderately sized split-valence basis set. These methods, though not exceptionally

sophisticated, are commonly used in QM calculations for large molecules, and will afford us a deeper understanding of the protein interaction.

#### *Facio FMO and GAMESS*

Facio FMO was developed by a group at Kyushu University in Japan for use in preparing fragment input files for GAMESS. Facio FMO provides a graphical user interface (GUI) with the capability to convert structural files into GAMESS input files for QM calculations. General Atomic and Molecular Electronic Structure System (GAMESS) was developed at Iowa State University that runs quantum mechanical calculations.

## ***Results***

### *MD Simulation Stability*

To ensure stability of the protein throughout the MD simulation, root-mean-square deviation (RMSD), radius of gyration, root-mean-square fluctuation (RMSF), and potential energy, were calculated in each frame. RMSD refers to the average distance in backbone atoms from the original structure to the current frame. The RMSD is expected to increase as the protein deviates further from its initial structure but should not expand rapidly, an indication of unfolding. The coefficient of variation for the RMSD of our system was consistently lower than 5% for the last 5,000 frames, indicating stability within the structure.

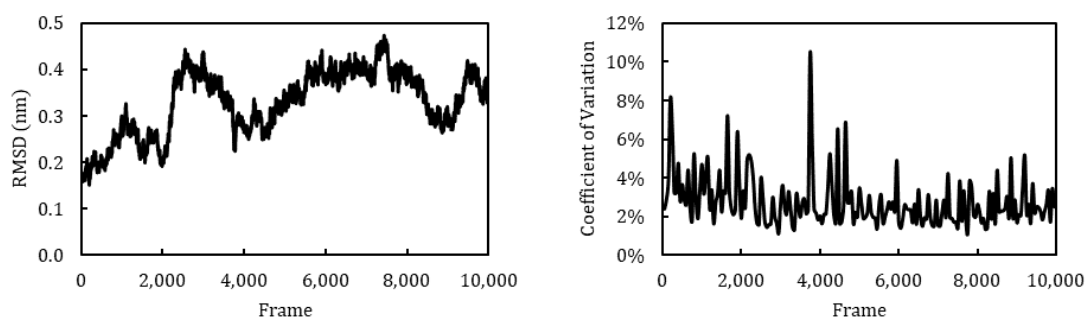


Figure 4. Root-mean-square deviation across total simulation time.

Figure 5. Coefficient of variation in RMSD across total simulation time.

Radius of gyration is another diagnostic tool used to determine the stability of the MD simulation. The radius of gyration refers to the root-mean-square distance of atoms from their mass-weighted center. Our results showed a fluctuation between 3.13 nm and 3.28 nm over a period of 20 ns. The coefficient of variation in the radius of gyration over time was below 0.5%, again indicating stability.



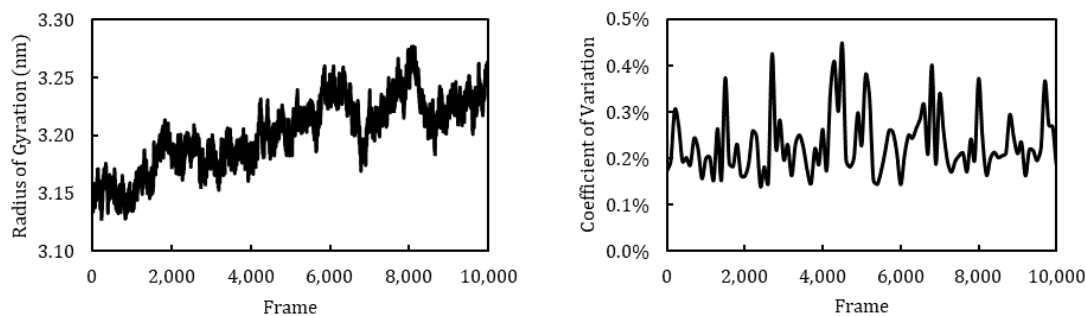


Figure 6. Radius of gyration across total simulation time.

Figure 7. Coefficient of variation in radius of gyration across total simulation time.

Root-mean-square fluctuation (RMSF) refers to the average deviation over time for each residue. Two major peaks, with fluctuation greater than 0.4 nm were identified for residue tags 448 and 734, which correspond to the N-terminal Arg-3 and C-terminal Lys-326 of IL-1RAcP, respectively. Protein termini are more prone to movement, thus the spike in RMSF was not considered unusual and did not signify a lack of stability in the simulation. All other residues remain below 0.4 nm distance fluctuation, thus indicating overall stability for the system.

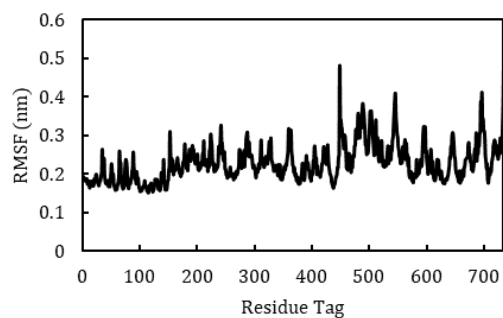


Figure 8. Average root-mean-square fluctuation for each residue throughout total simulation time.

Lastly, the potential energy was tracked over time. The NPT ensemble was used in the MD simulation to purposefully decrease and stabilize the potential energy into a PE well. The initial decline in PE was expected, indicating energy stabilization. The coefficient of variation over time was below 0.1%, which indicated energy equity among the equilibrated set of structures.

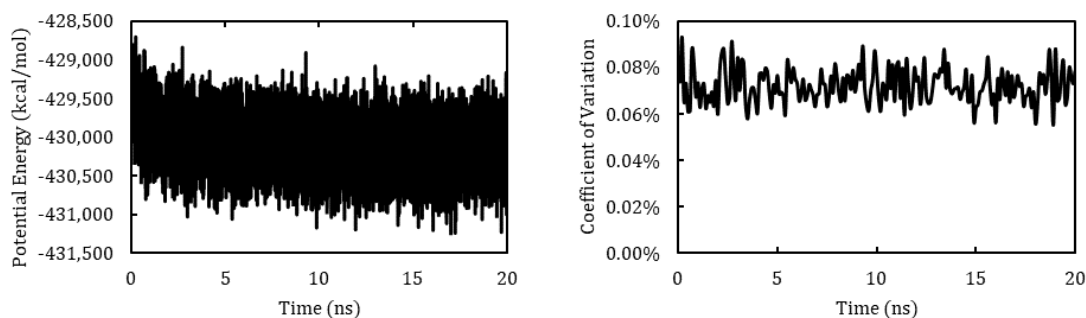


Figure 9. Potential energy across total simulation time.

Figure 10. Coefficient of variation in potential energy across total simulation time.

A stable MD simulation is critical to ensuring accurate post-simulation analysis, including MM-PBSA/GBSA. Thus, several diagnostic techniques were employed to track the stability of the protein system throughout the simulation time. The RMSD, radius of gyration, RMSF, and PE all indicated an appropriate MD simulation.

#### *MM-PBSA/GBSA Results*

Four possible binding regions were chosen through literature review and visual inspection of the protein structure. Then, MMPSBA/GBSA calculations were performed on the labeled residues of interest to determine which binding region, and ultimately which residue contributes the most to binding stability. The MM-PBSA/GBSA results were then decomposed to electrostatic (ES), van der Waals

(VDW), and polar (P) and nonpolar (NP) solvation energies as shown in the equation below:

$$\Delta G_{binding} = \Delta G^{ES} + \Delta G^{VDW} + \Delta G^{P,solv} + \Delta G^{NP,solv} \quad (5)$$

As expected, charged residues had large electrostatic contributions. High polar solvation energy was expected in residues with large negative electrostatic contributions to compensate for solvent interactions.

Arg-286 has the lowest total free energy of binding which is dominated by its electrostatic contribution. Asp-54 is a likely binding partner due to the residue orientation and low ES contribution. Thus, region I is an interesting target for further study.

Region IV has several residues with low total free energy of binding values but without a dominant type of interaction. This would indicate that the interaction among residues is more complex than simply a single electrostatic interaction between Arg-286 and Asp-54 holding the proteins together.

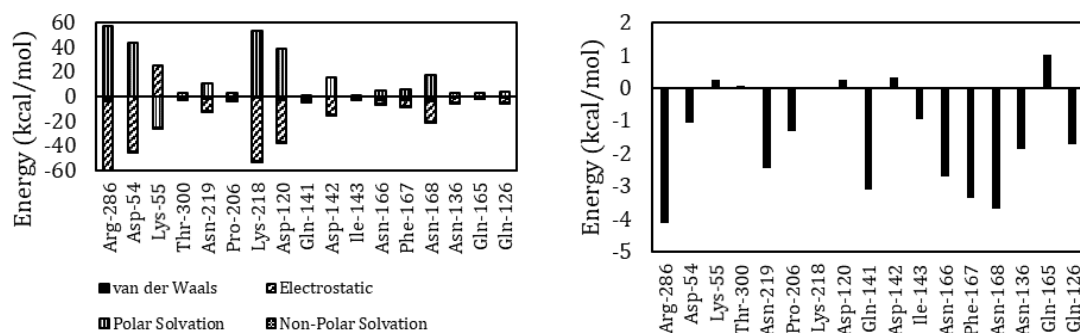


Figure 11. Decomposed free energy of binding for region I-IV residues.

Figure 12. Total free energy of binding for region I-IV residues.

Table 1. Binding regions and specific residues belonging to each.

Region	Residues	Protein
I	Arg-286	IL-1RAcP
	Asp-54, Lys-55	IL-1 $\beta$
	Thr-437	IL-1RI
II	Asn-219	IL-1RAcP
	Pro-206	IL-1RI
III	Lys-218	IL-1RAcP
	Asp-120	IL-1 $\beta$
IV	Gln-141, Asp-142, Ile-143, Gln-126	IL-1 $\beta$
	Asn-166, Phe-167, Asn-168, Gln-165	IL-1RAcP
	Asn-136	IL-1RI

Though several residues showed compelling free energy of binding values, Arg-286 had the lowest value and dominant electrostatic contribution, which is consistent with the work of Liotta and Luchini, who identified this residue as a “hot spot” for protein-protein interaction. Arg-286 was ultimately chosen for further

study using FMO methods to account for quantum mechanical contributions to binding.

### *FMO Results*

Residues within 0.5 nm of Arg-286 were chosen for FMO calculations. Each terminal residue was manually capped with a methyl group, creating N-met or acetyl for the N- and C-termini, respectively. The Facio software was then used to fragment segments longer than 2 amino acids into 1-2 residue components for the FMO QM calculations. QM calculations were performed in-vacuo as the binding region in question is not solvent accessible. The five lowest energy pair interactions are shown below. Among the five pairs, Arg-286 is involved in three separate interactions. Electrostatic and charge transfer interactions were dominant in those three pairs, as expected with a negatively charged residue. Pair 5 had lowest total interaction energy, composed mainly of electrostatic forces. This is likely due to an interaction between Arg-286 of fragment 1 and Asp-54 of fragment 2.

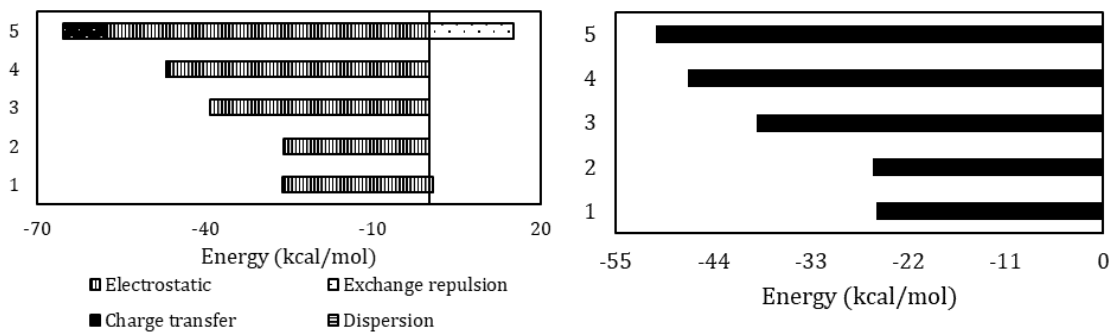


Figure 13. Decomposed pair interaction energy for pairs 1-5.

Figure 14. Total pair interaction energy for pairs 1-5.

Table 2. Residues belonging to pairs 1-5.

Pair Number	Fragment 1 (IL-1RAcP)	Fragment 2 (IL-1 $\beta$ )
5	Arg-286, Thr-287	Asp-54, Lys-55
4	Arg-286, Thr-287	Glu-111
3	Glu-288, Asp-289	Lys-138
2	Lys-212	Glu-111
1	Arg-286, Thr-287	Glu-105, Ile-106

### *Hydrogen Bond Analysis*

Hydrogen bond analysis in Chimera shows a hydrogen bond between Arg-286 and Asp-54 with a distance of 1.63 Å. Chimera identifies hydrogen bonds by locating bond donors within 5 Å of acceptors. Hydrogen bonds are largely

electrostatic in nature, which would explain the electrostatic contribution of Arg-286 as seen in MM-PBSA/GBSA and FMO calculations.

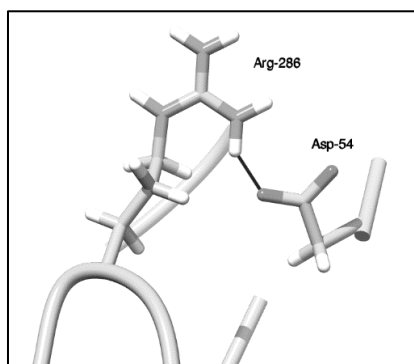


Figure 15. Hydrogen bond between Arg-286 (IL-1RAcP) and Asp-54 (IL-1 $\beta$ ) as identified in Chimera.



## ***Conclusion***

As hypothesized, MD simulations/MM calculations reproduced the experimental results with respect to Arg-286 being the 'hot spot' residue for the IL-1 $\beta$ :IL-1RI:IL-1RAcP complex formation. FMO methods suggest that electrostatic interactions contribute most to the stabilizing interactions between Arg-286 and neighboring residues. Hydrogen-bond analysis, in conjunction with the MM-PBSA/GBSA and FMO results, suggest that a hydrogen bond between Arg-286 of IL-1RAcP and Asp-54 of IL-1 $\beta$  contribute significantly to the stability of the IL-1 $\beta$  ternary complex. Overall, in agreement with the experimental protein painting results from the Liotta and Luchini labs, the interaction between Arg-286 and Asp-54 were identified as potential targets for drug discovery with the aim of preventing IL-1 $\beta$  complex formation and thereby inhibition of subsequent downstream inflammatory effects.

## ***Methods***

This section contains a basic overview of the programs used in running all calculations. See appendix for submit scripts and input files relating to the parenthetical numbers located in this section.

### *Hardware/Software*

MD and QM calculations were performed on the ARGO cluster at George Mason University. The ARGO Cluster is a batch computing resource assembled at the Krasnow Institute in 2013 by the Office of Research Computing. ARGO contains 64 Dell Compute Nodes that support parallel computing. To submit jobs to the ARGO cluster, submit scripts were sent to the slurm workload manager (1).

Chimera 1.11.2 was used for initial structure editing, visualization, and hydrogen bond analysis. Amber14, located on the ARGO cluster, was used for all MD simulations and MM calculations. Facio 20.1.3 was used for preparation of FMO input files and FMO output analysis. GAMESS, released April 20, 2017, also located on the ARGO cluster, was used for all QM calculations.

### *Initial Editing*

The initial IL-1 $\beta$  ternary complex structure file was obtained from the RCSB Protein Data Bank with a PDB ID of 4DEP. Chimera editing software was used to prepare the PDB file for use in AmberMD. Using Chimera, the residues were completed using the Dunbrack rotamer library and hydrogen atoms were added. Then, using the Chimera interface for Modeller, two long bonds ( $> 10 \text{ \AA}$ ) located in loop structures were refined to provide a more realistic structure.

### *MD and MM-PBSA/GBSA in Amber*

After editing in Chimera, the final PDB file was loaded into Amber using tLeaP and the ff14SB force field. The protein system was solvated using the TIP3P water model in a  $12.0 \text{ \AA}$  box and the overall  $-2.0$  charge was neutralized with sodium ions. Coordinate and topology files were saved in solvated and unsolvated forms for the following structure files: total complex, IL-1 $\beta$ /IL-1RI, and IL-1RAcP, for use in MM-PBSA/GBSA calculations.

Next, pmemd was used to minimize the solvated complex with the NVT ensemble. Initially, only the solvent was minimized to remove any bad contacts formed in solvation (2). Next, the entire system was minimized to relax the crystal structure of the ternary complex (3).

Following minimization, six serial equilibrations were run for a total equilibration time of 20 ns at 300 K and 1 bar, using the NPT ensemble under periodic boundary conditions (4). To analyze the stability of the MD simulation,

cpptraj was used with the functions rms, radgyr, and rmsf for RMSD, radius of gyration, and RMSF, respectively. Potential energy was isolated from the pmemd output file using a perl script retrieved from an online Amber tutorial.

A short production run of 50 frames followed the long equilibration (10,000 frames) step to provide a small and equilibrated input for MM-PBSA/GBSA calculations (5).

MM-PBSA/GBSA calculations were performed using per-residue decomposition (6). The restriction in number of nodes required for MM-PBSA/GBSA calculations also restricted the amount of available memory for the calculations. For this reason, more robust systems must forgo PB calculations in favor of the more streamlined GB calculations.

#### *FMO and GAMESS*

Chimera software was used to identify residues within 5.0 Å of Arg-286 with the zone tool. Once the residues were identified, the residues were isolated and capped with an N-met and acetyl groups, manually.

The fragment file was loaded into Facio and the initial fractioning points were determined in the FMO 5.2 GAMESS control panel. The peptides were further fragmented if necessary leaving no larger than a 2-residue fragment. Then, the group member and charge for each fragment were identified and the FMO input parameters were set and the input file was saved for use in GAMESS (7).

The prepared input file was run in GAMESS across 4 nodes and the output file was analyzed in Facio.

## Appendix

### (1) General submit script

```
#!/bin/bash
#SBATCH --job-name=REVA
#SBATCH -o /scratch/rjoshi10/slurm-%N-%j.out
#SBATCH -e /scratch/rjoshi10/slurm-%N-%j.err
#SBATCH --mail-user=rjoshi10@gmu.edu
#SBATCH --mail-type=BEGIN,END,FAIL,REQUEUE,TIMELIMIT_80
#SBATCH --partition=all-LoPri
#SBATCH --mem=8000
#SBATCH --time=5-00:00:00
#SBATCH --export=NONE
#SBATCH --nodes=4
#SBATCH --ntasks-per-node=8
module load mpich/ge/intel/64/3.2
module load amber/intel/16
##
export OMP_NUM_THREADS=1
## Run the executable
mpirun -np 32 pmemd.MPI -o -i equil.in -o equil_06.out -p 4dep_solv.prmtop -c
equil_05.rst -r equil_06.rst -x equil_06.mdcrd -inf mdinfo -l logfile; \
```

### (2) Initial solvent/ion minimization

```
Solvent-ion minimization
&cntrl
  imin = 1,
  maxcyc = 2500,
  ncyc = 1000,
  ntb = 1,
  ntr = 1,
  cut = 10.0
&end
Group input for restrained atoms
100.0
RES 1 791
END
END
```

### (3) Total protein system minimization

```
System minimization
&cntrl
  imin = 1,
  maxcyc = 2500,
  ncyc = 1000,
  ntb = 1,
  ntr = 0,
  cut = 10.0,
  ntp = 50,
  ntso = 2,
&end
```

### (4) Equilibration

```
heat 4dep
&cntrl
  imin=0, irest=1, ntx=5,
  nstlim=2000000, dt=0.002,
  ntc=2, ntf=2,
  cut=8.0, ntb=2, ntp=1, taup=2.0,
  ntr=1000, ntwx=1000,
  ntt=3, gamma_ln=2.0,
  temp0=300.0, ig=-1,
/
```

### (5) Production

```
heat 4dep
&cntrl
  imin=0, irest=1, ntx=5,
  nstlim=1000, dt=0.002,
  ntc=2, ntf=2,
  cut=8.0, ntb=2, ntp=1, taup=2.0,
  ntr=50, ntwx=50,
  ntt=3, gamma_ln=2.0,
  temp0=300.0, ig=-1,
/
```

### (6) MM-PBSA/GBSA Input

```
Per-residue GB and PB decomposition
&general
  endframe=50, verbose=1,
/
&gb
  igb=5, saltcon=0.100,
/
&pb
  istrng=0.100,
/
&decomp
  idecomp=1, print_res="14; 126; 140-143; 299-304; 355; 580; 613; 625-626; 674;
707"
  dec_verbose=1,
/
```

## (7) GAMESS FMO input

```
!*** FMO 5.2 (Gamess) INPUT generated by Facio 20.1.3 ***
$CONTRL RUNTYP=ENERGY NPRINT=-5 ISPHER=-1 MAXIT=80 $END
$SYSTEM MWORDS=250 $END
$GDDI NGROUP=4 $END
$INTGRL NINTIC=-9000000 $END
$SCF DIRSCF=.t. diis=.t. damp=.t. soscf=.f. NPUNCH=0 conv=1e-6 $END
!*** NumCPU : 2 MemPerNode : 512MB
$PCM SOLVNT=WATER IEF=-10 ICOMP=2 ICAV=1 IDISP=1 IFMO=2 $END
$PCMAV RADII=SUAHF $END
$TESCAV NTSALL=60 $END
$FMOPRP
  NAODIR=210
  NGRFMO(1)=4, 4, 0, 0, 0, 0, 0, 0, 0, 0
  IPIEDA=1
  NPRINT=9
  NPCMIT=2
$END
$FMO
  SCFTYP(1)=RHF
  MODGRD=10
  MODMUL=0
  MAXCAO=5
  MAXBND=8
  NLAYER=1
  NFRAG=16
  ICHARG(1)= 0, 0, -1, -1, 0, 1, 0, 0, 0, 0,
             1, 0, 0, 0, 1, -2
  FRGNAM(1)= Frag1, Ile-3, Frag2, Glu-6, Tyr-7,
             Lys-8, Thr-9, His-10, Frag3, Asn-13,
             Lys-13, Frag4, Gly-15, Frag5, Frag6,
             Frag7
  INDAT(1)= 0
             1 -46 0
             47 -69 0
             70 -111 0
             112 -138 0
             139 -171 0
             172 -205 0
             206 -223 0
             224 -248 0
             249 -282 0
             283 -318 0
             319 -344 0
             345 -376 0
             377 -391 0
             392 -423 0
             424 -461 0
             462 -496 0
$END
$FMOHYB
6-31G 9 5
1 0 -0.067723 0.300280 0.000000 0.000000 0.606750
    0.306535 0.000000 0.000000 0.309792
0 1 -0.067730 0.300309 0.572036 0.000000 -0.202233
    0.306551 0.292061 0.000000 -0.103255
0 1 -0.067730 0.300309 -0.286018 -0.495398 -0.202233
    0.306551 -0.146031 -0.252932 -0.103255
0 1 -0.067730 0.300309 -0.286018 0.495398 -0.202233
    0.306551 -0.146031 0.252932 -0.103255
0 1 1.011953 -0.016447 0.000000 0.000000 0.000000
    -0.059374 0.000000 0.000000 -0.000000
MINI 5 5
1 0 -0.104883 0.308874 0.000000 0.000000 0.521806
```



0 1	-0.104883	0.308874	0.491961	0.000000	-0.173934
0 1	-0.104883	0.308876	-0.245980	-0.426050	-0.173933
0 1	-0.104883	0.308876	-0.245980	0.426050	-0.173933
0 1	0.988209	0.063992	0.000000	0.000000	0.000000

\$END  
\$FMOBND  
-55           70   6-31G       MINI  
-214          224   6-31G       MINI  
-276          283   6-31G       MINI  
-327          345   6-31G       MINI  
-365          377   6-31G       MINI  
-417          424   6-31G       MINI  
-452          462   6-31G       MINI

\$END  
\$DATA  
FMO calculation : frag\_min\_renum\_het.pdb  
C1  
H.1-1        1  
          N31 6  
  
C.1-1        6  
          N31 6  
  
O.1-1        8  
          N31 6  
  
N.1-1        7  
          N31 6  
  
\$END

## References

- Eisenberg, S., Evans, R., Arend, W., Verderber, E., Brewer, M., Hannum, C., & Thompson, R. (1990). Primary structure and functional expression from complementary DNA of a human interleukin-1 receptor antagonist. *Nature*, 343(6256), 341–346. <https://doi.org/10.1038/343341a0>
- Huang, J., Gao, X., Li, S., & Cao, Z. (1997). Recruitment of IRAK to the interleukin 1 receptor complex requires interleukin 1 receptor accessory protein. *Proceedings of the National Academy of Sciences of the United States of America*, 94(24), 12829–12832. <https://doi.org/10.1073/PNAS.94.24.12829>
- Thomas, C., Bazan, J. F., & Garcia, K. C. (2012). Structure of the activating IL-1 receptor signaling complex. *Nature Structural & Molecular Biology*, 19(4), 455–457. <https://doi.org/10.1038/nsmb.2260>
- Salomon-Ferrer, R., Case, D. A., & Walker, R. C. (2013). An overview of the Amber biomolecular simulation package. *Wiley Interdisciplinary Reviews: Computational Molecular Science*, 3(2), 198–210. <https://doi.org/10.1002/wcms.1121>
- Allen, M. P. (2004). Introduction to Molecular Dynamics Simulation. *Computing*, 23, 27. <https://doi.org/10.1016/j.cplett.2006.06.020>
- Case, D. A., Cheatham, T. E., Darden, T., Gohlke, H., Luo, R., Merz, K. M., ... Woods, R. J. (2005). The Amber biomolecular simulation programs. *Journal of Computational Chemistry*. <https://doi.org/10.1002/jcc.20290>
- Zhou, S., Liu, X., An, X., Yao, X., & Liu, H. (2017). Molecular Dynamics Simulation Study on the Binding and Stabilization Mechanism of Antiprion Compounds to the “hot Spot” Region of PrPC. *ACS Chemical Neuroscience*, 8(11), 2446–2456. <https://doi.org/10.1021/acscchemneuro.7b00214>

- Homeyer, N., & Gohlke, H. (2012). Free energy calculations by the Molecular Mechanics Poisson-Boltzmann Surface Area method. *Molecular Informatics*, *31*(2), 114–122. <https://doi.org/10.1002/minf.201100135>
- Maier, J. A., Martinez, C., Kasavajhala, K., Wickstrom, L., Hauser, K. E., & Simmerling, C. (2015). ff14SB: Improving the Accuracy of Protein Side Chain and Backbone Parameters from ff99SB. *Journal of Chemical Theory and Computation*, *11*(8), 3696–3713. <https://doi.org/10.1021/acs.jctc.5b00255>
- Heifetz, A., Chudyk, E. I., Gleave, L., Aldeghi, M., Cherezov, V., Fedorov, D. G., ... Bodkin, M. J. (2016). The Fragment Molecular Orbital Method Reveals New Insight into the Chemical Nature of GPCR-Ligand Interactions. *Journal of Chemical Information and Modeling*, *56*(1), 159–172. <https://doi.org/10.1021/acs.jcim.5b00644>
- Fedorov, D. G., & Kitaura, K. (2007). Pair interaction energy decomposition analysis. *Journal of Computational Chemistry*, *28*(1), 222–237. <https://doi.org/10.1002/jcc.20496>
- Izairi, R., & Kamberaj, H. (2017). Comparison Study of Polar and Nonpolar Contributions to Solvation Free Energy. *Journal of Chemical Information and Modeling*, *57*(10), 2539–2553. <https://doi.org/10.1021/acs.jcim.7b00368>
- Fedorov, D. G., & Kitaura, K. (2007). Extending the Power of Quantum Chemistry to Large Systems with the Fragment Molecular Orbital Method. *J. Phys. Chem. A*, *111*, 6904–6914. <https://doi.org/10.1021/jp0716740>
- Fedorov, D., Kitaura, K. (2009) *The Fragment Molecular Orbital Method: Practical Applications to Large Molecular Systems*. Boca Raton, Florida: CRC Press.

## ***Biography***

Reva S. Joshi received her Bachelor of Science in Chemistry with a concentration in Biochemistry from the Honor's College at Virginia Commonwealth University in 2016. During her two years at George Mason University, Reva worked as a Graduate Teaching Assistant while taking classes and participating in research. After completing her Master of Science degree in Chemistry, with a concentration in Biochemistry, she will go on to study medicine at Eastern Virginia Medical School in Norfolk, Virginia.